

# Linear Transceiver Design for Full-Duplex Multi-cell MIMO Systems

Ali Cagatay Cirik, *Member, IEEE*, Omid Taghizadeh, *Student Member, IEEE*, Lutz Lampe, *Senior Member, IEEE*, Rudolf Mathar, *Member, IEEE*, and Yingbo Hua, *Fellow, IEEE*

**Abstract**—We consider a multi-cell multiple-input multiple-output (MIMO) full-duplex (FD) system, where multiple FD capable base-stations (BSs) serve multiple mobile users operating in FD mode. The self-interference at the BSs and users, and co-channel interference (CCI) between all the nodes (BSs and users) in the system are both taken into account. We consider the transmit and receive filter design for sum-rate maximization problem subject to sum-power constraints at the BSs and individual power constraints at each user of the system under the limited dynamic range considerations at the transmitters and receivers. By reformulating this non-convex problem as an equivalent multi-convex optimization problem with the addition of two auxiliary variables, we propose a low complexity alternating algorithm which converges to a stationary point. Since this sum-rate maximization results in starvation of users in terms of resources depending on the power of the self-interference and CCI channels, we modify the sum-rate maximization problem by adding target data rate constraints on each user, and propose an algorithm based on Lagrangian relaxation of the rate constraints.

**Keywords**—Full-duplex, MIMO, multi-cell, self interference, transceiver designs.

## I. INTRODUCTION

IN current half-duplex (HD) cellular systems, uplink (UL) and downlink (DL) channels are designed to operate in either separate time slots or separate frequency bands, resulting in inefficient usage of the radio resources. Full-duplex (FD) systems, which enable simultaneous transmission and reception at the same time in the same frequency band, have recently gained considerable interest, e.g., for their potential to improve spectral efficiency of the next generation wireless communication systems [1]-[5].

The introduction of FD base-stations (BSs) introduce not only self-interference, but also co-channel interference (CCI) from UL users to DL users. FD communication has been investigated for single cell systems in [6]-[8]. However the authors in [6]-[8] ignore several fundamental impediments of

FD systems, i.e. transmitter and receiver distortion caused by non-ideal amplifiers, oscillators, analog-to-digital converters (ADCs), and digital-to-analog converters (DACs), etc. [9] and thus several system parameters were ideally assumed.

In this paper, we consider a multi-cell FD multiple-input multiple-output (MIMO) scenario where FD capable BSs communicate with mobile users operating in FD mode at the same time slot over the same frequency band. In addition to self-interference channel at the BSs and users, the CCI between all the nodes in the system is also taken into account, which increases the difficulty of the optimization problem further. The sum-rate maximization problem for this system subject to sum-power constraints at the BSs and individual power constraints at each user of the system is studied under the practical FD impairments.

By introducing two auxiliary variables, the non-convex sum-rate maximization problem is reformulated as an equivalent multi-convex problem [10], [11], and a low complexity algorithm that converges to a stationary point is developed. In [8] and [12], sum-rate maximization problem in FD single-cell MIMO systems has been considered, where the relationship between weighted-sum-rate and weighted minimum-mean-squared-error (WMMSE) problems [13], [14] is exploited to solve the sum-rate maximization problem. Different from [8], [12], where this relationship only holds when the receivers employ minimum-mean-squared-error (MMSE) receive filter, the proposed algorithm in this paper exploits the same relationship under any kind of receive filters. Moreover, the introduction of auxiliary variables makes the domain of the problem larger than the domain of the WMMSE approach [8], [12], and thus the proposed solution always achieves equal or higher sum-rate than WMMSE algorithm.

Moreover, the works [6]-[8] and [12] consider the sum-rate maximization problem in a single-cell FD system without rate constraints, which generally results in an unfair resource allocation. Users with favorable link conditions get most of the resources, whereas the other users are deprived of resources. For example, as shown in [6], [15], as the self-interference power increases, all the resources are devoted to downlink (DL) system to maximize the sum-rate, and uplink (UL) users are not served. Therefore, to introduce fairness, we include data rate constraints as a quality-of-service (QoS) constraint, and solve the problem of sum-rate maximization subject to data rate and power constraints by exploiting the Lagrangian relaxation of the rate constraints [16].

Simulation results demonstrate that for both single and multi-cell small-cell systems, the sum-rate achieved by the

---

A. C. Cirik and L. Lampe are with the Department of Electrical and Computer Engineering, University of British Columbia, Vancouver, BC V6T 1Z4, Canada (email: {cirik, lampe}@ece.ubc.ca).

O. Taghizadeh and R. Mathar are with the Institute for Theoretical Information Technology, RWTH Aachen University, Aachen, 52074, Germany (email: {taghizadeh, mathar}@ti.rwth-aachen.de).

Y. Hua is with the Department of Electrical Engineering, University of California, Riverside, CA 92521, USA (email: yhua@ece.ucr.edu).

Part of this work will be presented in IEEE 84th Vehicular Technology Conference (VTC), Montreal, Canada, September 2016. This work was supported in part by the Natural Sciences and Engineering Research Council of Canada (NSERC).

FD mode is higher than that of baseline HD scheme as the capability of current self-interference cancellation schemes is efficient, which shows that FD is a promising technique to improve the spectral efficiency of small cell wireless communication systems.

### A. Notations

Before proceeding, we would like to introduce notation used in the following. Matrices and vectors are denoted as bold capital and lowercase letters, respectively.  $(\cdot)^T$  is the transpose;  $(\cdot)^H$  is the conjugate transpose;  $\mathbb{E}\{\cdot\}$  means the statistical expectation;  $\mathbf{I}_N$  is the  $N$  by  $N$  identity matrix;  $\mathbf{0}_{N \times M}$  is the  $N$  by  $M$  zero matrix;  $\text{tr}(\cdot)$  is the trace;  $\text{Cov}\{\cdot\}$  is the covariance;  $|\cdot|$  is the determinant;  $\text{diag}(\mathbf{A})$  is the diagonal matrix with the same diagonal elements as  $\mathbf{A}$ ,  $[\mathbf{A}]_{nn}$  denotes the  $n$ th row and  $n$ th column of matrix  $\mathbf{A}$ .  $\mathcal{CN}(\mu, \sigma^2)$  denotes a complex Gaussian distribution with mean  $\mu$  and variance  $\sigma^2$ .  $\mathbb{C}^{N \times M}$  denotes the set of complex matrices with a dimension of  $N$  by  $M$ .  $\perp$  denotes the statistical independence.  $(x)^+ = \max(x, 0)$ .

## II. SYSTEM MODEL

In this section, we describe the system model of a multi-cell MIMO system consisting of FD BSs and FD users as seen in Fig. 1. In addition to well-known interference sources in traditional multi-cell HD systems, i.e., from UL users to BSs and from BSs to DL users, incorporating FD empowered BSs and users to traditional HD cellular systems introduces new sources of interference due to simultaneous transmission and reception at all the nodes in the system, 1) the self-interference at each FD BSs and users, 2) the interference among adjacent BSs, i.e., inter-BS interference, 3) CCI among the all users in all cells.

We consider a  $K$  cell FD system, where BS  $k$ ,  $k = 1, \dots, K$  is equipped with  $M_k$  transmit and  $N_k$  receive antennas, and serves  $I_k$  users in cell  $k$ . We denote  $i_k$  to be the  $i$ th user in cell  $k$  with  $M_{i_k}$  transmit and  $N_{i_k}$  receive antennas. We define the set of all BSs as  $\mathcal{K} = \{k \in \{1, \dots, K\}\}$  and all users as  $\mathcal{I}$  given by

$$\mathcal{I} = \{i_k \mid k \in \{1, 2, \dots, K\}, i \in \{1, 2, \dots, I_k\}\}.$$

Let us denote  $\mathbf{H}_{kl_j}^{UL} \in \mathbb{C}^{N_k \times M_{l_j}}$  as the channel between BS  $k$  and user  $l_j$  in the UL channel,  $\mathbf{H}_{i_k j}^{DL} \in \mathbb{C}^{N_{i_k} \times M_j}$  as the channel between BS  $j$  and user  $i_k$  in the DL channel,  $\mathbf{H}_{i_k l_j}^{UU} \in \mathbb{C}^{N_{i_k} \times M_{l_j}}$  as the CCI channel from the user  $l_j$  to the user  $i_k$ ,  $\mathbf{H}_{kj}^{BB} \in \mathbb{C}^{N_k \times M_j}$  as the inter-BS interference channel from the BS  $j$  to the BS  $k$ ,  $\mathbf{H}_k^{SI} \in \mathbb{C}^{N_k \times M_k}$  as the self-interference channel from the transmitter to the receiver antennas of BS  $k$ , and  $\mathbf{H}_{i_k}^{SI} \in \mathbb{C}^{N_{i_k} \times M_{i_k}}$  as the self-interference channel from the transmitter to the receiver antennas of user  $i_k$ .

We also take into account the limited dynamic range (DR), which is caused by non-ideal amplifiers, oscillators, ADCs, and DACs. We adopt the limited DR model in [9], which has also been commonly used in [15]-[20]. Particularly, at each receive antenna an additive white Gaussian ‘‘receiver distortion’’ with variance  $\beta$  times the energy of the undistorted received signal

on that receive antenna is applied, and at each transmit antenna, an additive white Gaussian ‘‘transmitter noise’’ with variance  $\kappa$  times the energy of the intended transmit signal is applied. This transmitter/receiver distortion model is valid, since it was shown by hardware measurements in [21] and [22] that the non-ideality of the transmitter and receiver chain can be approximated by an independent Gaussian noise model, respectively.

The source symbols of the user  $i_k$  in the UL and DL channel are denoted as  $s_{i_k}^{UL}$  and  $s_{i_k}^{DL}$ , and they are both assumed to have unit powers. Denoting the precoders for the data stream of user  $i_k$  as  $\mathbf{v}_{i_k}^{UL} \in \mathbb{C}^{M_{i_k} \times 1}$  in the UL channel, and  $\mathbf{v}_{i_k}^{DL} \in \mathbb{C}^{M_k \times 1}$  in the DL channel, the transmitted signal of the user  $i_k$  and that of the BS  $k$  can be written, respectively, as

$$\mathbf{x}_{i_k}^{UL} = \mathbf{v}_{i_k}^{UL} s_{i_k}^{UL}, \quad (1)$$

$$\mathbf{x}_k^{DL} = \sum_{i=1}^{I_k} \mathbf{v}_{i_k}^{DL} s_{i_k}^{DL}. \quad (2)$$

The signal received by the BS  $k$  and that received by the user  $i_k$  can be written, respectively, as

$$\begin{aligned} \mathbf{y}_k^{UL} = & \sum_{i=1}^{I_k} \mathbf{H}_{ki_k}^{UL} (\mathbf{x}_{i_k}^{UL} + \mathbf{c}_{i_k}^{UL}) + \mathbf{H}_k^{SI} (\mathbf{x}_k^{DL} + \mathbf{c}_k^{DL}) \\ & + \sum_{j=1, j \neq k}^K \mathbf{H}_{kj}^{BB} (\mathbf{x}_j^{DL} + \mathbf{c}_j^{DL}) + \mathbf{e}_k^{UL} \\ & + \sum_{j=1, j \neq k}^K \sum_{l=1}^{I_j} \mathbf{H}_{kl_j}^{UL} (\mathbf{x}_{l_j}^{UL} + \mathbf{c}_{l_j}^{UL}) + \mathbf{n}_k^{UL}, \end{aligned} \quad (3)$$

$$\begin{aligned} \mathbf{y}_{i_k}^{DL} = & \mathbf{H}_{i_k k}^{DL} (\mathbf{x}_k^{DL} + \mathbf{c}_k^{DL}) + \mathbf{H}_{i_k}^{SI} (\mathbf{x}_{i_k}^{UL} + \mathbf{c}_{i_k}^{UL}) \\ & + \sum_{(l,j) \neq (i,k)} \mathbf{H}_{i_k l_j}^{UU} (\mathbf{x}_{l_j}^{UL} + \mathbf{c}_{l_j}^{UL}) + \mathbf{e}_{i_k}^{DL} \\ & + \sum_{j=1, j \neq k}^K \mathbf{H}_{i_k j}^{DL} (\mathbf{x}_j^{DL} + \mathbf{c}_j^{DL}) + \mathbf{n}_{i_k}^{DL}, \end{aligned} \quad (4)$$

where  $\mathbf{n}_k^{UL} \sim \mathcal{CN}(\mathbf{0}_{N_k}, \sigma_k^2 \mathbf{I}_{N_k})$  and  $\mathbf{n}_{i_k}^{DL} \sim \mathcal{CN}(\mathbf{0}_{N_{i_k}}, \sigma_{i_k}^2 \mathbf{I}_{N_{i_k}})$  denote the additive white Gaussian noise (AWGN) vectors at the BS  $k$  and user  $i_k$ , respectively.

Moreover, in (3),  $\mathbf{c}_{i_k}^{UL} \in \mathbb{C}^{M_{i_k}}$  is the transmitter noise at the transmitter antennas of user  $i_k$ , which models the effect of limited transmitter DR and closely approximates the effects of additive power-amplifier noise, non-linearities in the DAC and phase noise. The covariance matrix of  $\mathbf{c}_{i_k}^{UL}$  is given by  $\kappa$  times the energy of the intended signal at each transmit antenna, In particular  $\mathbf{c}_{i_k}^{UL}$  can be modeled as [9]

$$\mathbf{c}_{i_k}^{UL} \sim \mathcal{CN}(\mathbf{0}, \kappa \text{diag}(\mathbf{v}_{i_k}^{UL} (\mathbf{v}_{i_k}^{UL})^H)), \quad (5)$$

$$\mathbf{c}_{i_k}^{UL} \perp \mathbf{x}_{i_k}^{UL}. \quad (6)$$

Finally, in (4),  $\mathbf{e}_{i_k}^{DL} \in \mathbb{C}^{N_{i_k}}$  is the additive receiver distortion at the  $i_k$ -th user, which models the effect of limited receiver DR and closely approximates the combined effects of additive gain-control noise, non-linearities in the ADC and

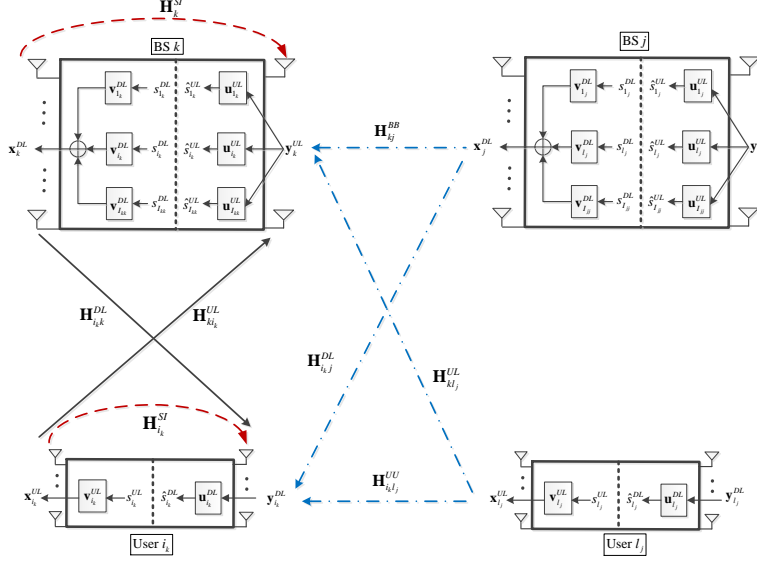


Fig. 1. FD MIMO multi-cell system. For simplicity, we depict two cells, and one user in each cell.

phase noise. The covariance matrix of  $\mathbf{e}_{i_k}^{DL}$  is given by  $\beta$  times the energy of the undistorted received signal at each receive antenna. In particular,  $\mathbf{e}_{i_k}^{DL}$  can be modeled as [9]

$$\mathbf{e}_{i_k}^{DL} \sim \mathcal{CN}(\mathbf{0}, \beta \text{diag}(\Phi_{i_k}^{DL})), \quad (7)$$

$$\mathbf{e}_{i_k}^{DL} \perp \mathbf{p}_{i_k}^{DL}, \quad (8)$$

where  $\Phi_{i_k}^{DL} = \text{Cov}\{\mathbf{p}_{i_k}^{DL}\}$ , and  $\mathbf{p}_{i_k}^{DL}$  is the  $i_k$ -th user's undistorted received vector, i.e.  $\mathbf{p}_{i_k}^{DL} = \mathbf{y}_{i_k}^{DL} - \mathbf{e}_{i_k}^{DL}$ . The discussion on the transmitter/receiver distortion holds for  $\mathbf{c}_k^{DL}$  and  $\mathbf{e}_k^{UL}$  as well.

The received signals are processed by linear decoders, denoted as  $\mathbf{u}_{i_k}^{UL} \in \mathbb{C}^{N_k \times 1}$ , and  $\mathbf{u}_{i_k}^{DL} \in \mathbb{C}^{N_{i_k} \times 1}$  by the BS  $k$  and the user  $i_k$ , respectively. Therefore, the estimates of data stream of user  $i_k$  in the UL and DL channels are given as

$$\hat{\mathbf{s}}_{i_k}^{UL} = (\mathbf{u}_{i_k}^{UL})^H \mathbf{y}_{i_k}^{UL}, \quad (9)$$

$$\hat{\mathbf{s}}_{i_k}^{DL} = (\mathbf{u}_{i_k}^{DL})^H \mathbf{y}_{i_k}^{DL}. \quad (10)$$

Using these estimates, the signal-to-interference-plus-noise ratio (SINR) of user  $i_k$  in the UL and DL channel can be expressed, respectively, as

$$\gamma_{i_k}^X = \frac{|(\mathbf{u}_{i_k}^X)^H \mathbf{H}_{i_k}^X \mathbf{v}_{i_k}^X|^2}{(\mathbf{u}_{i_k}^X)^H \Sigma_{i_k}^X \mathbf{u}_{i_k}^X}, \quad i_k \in \mathcal{I}, \quad X \in \{UL, DL\}, \quad (11)$$

where the covariance matrix of aggregate interference-plus-noise for the user  $i_k$  in the UL channel,  $\Sigma_{i_k}^{UL}$  and in the DL channel,  $\Sigma_{i_k}^{DL}$  can be approximated, under  $\beta \ll 1$  and  $\kappa \ll 1$ , as in (12) and (13), respectively, given at the bottom of the following page. Here,  $\mathbf{H}_{i_k}^X$  represents:

$$\mathbf{H}_{i_k}^X = \begin{cases} \mathbf{H}_{k i_k}^{UL}, & \text{if } X = UL, \\ \mathbf{H}_{i_k k}^{DL}, & \text{if } X = DL. \end{cases}$$

The sum-rate maximization problem can be formulated as:

$$\max_{\mathbf{v}, \mathbf{u}} \sum_{X \in \{UL, DL\}} \sum_{k=1}^K \sum_{i=1}^{I_k} \log_2(1 + \gamma_{i_k}^X) \quad (14)$$

$$\text{s.t.} \quad (\mathbf{v}_{i_k}^{UL})^H \mathbf{v}_{i_k}^{UL} \leq P_{i_k}, \quad i_k \in \mathcal{I}, \quad (15)$$

$$\sum_{i=1}^{I_k} (\mathbf{v}_{i_k}^{DL})^H \mathbf{v}_{i_k}^{DL} \leq P_k, \quad k \in \mathcal{K}, \quad (16)$$

where  $P_{i_k}$  in (15) is the transmit power constraint at the user  $i_k$ , and  $P_k$  in (16) is the total power constraint at the BS  $k$ . The optimization variables  $\mathbf{v}(\mathbf{u})$  denote the set of all transmit (receive) beamforming vectors, i.e.,  $\mathbf{v}(\mathbf{u}) = \{\mathbf{v}_{i_k}^X(\mathbf{u}_{i_k}^X) : i_k \in \mathcal{I}, X \in \{UL, DL\}\}$ .

The optimization problem (14)-(16) can be solved using the WMMSE approach [8], [12]-[14], which exploits the relationship between WSR and WMMSE optimization problems. This relationship holds only when the receivers use MMSE receive filters [13]. Recently, multi-convex approach has been introduced, which is shown to outperform WMMSE approach in terms of complexity and performance [11]. In the next subsection, we will exploit this multi-convex formulation to establish the WSR and WMMSE relationship for any arbitrary transmit and receive filters in FD multi-cell systems. Moreover, the domain of our objective function is larger than the domain of the WMMSE approach [8], [12] because of the additional auxiliary variables introduced by the proposed approach. This means that even though the initializations of the two problems are same, they will generally converge to different stationary

points. In particular, proposed algorithm achieves always equal or higher sum-rate than that of WMMSE algorithm [11].

### A. Multi-Convex Optimization

We first define a function

$$\begin{aligned} \psi_{i_k}^X &= \frac{\mathbb{E} \left\{ |w_{i_k}^X s_{i_k}^X|^2 \right\}}{\mathbb{E} \left\{ |\hat{s}_{i_k}^X - w_{i_k}^X s_{i_k}^X|^2 \right\}} \\ &= \frac{|w_{i_k}^X|^2}{\left| (\mathbf{u}_{i_k}^X)^H \mathbf{H}_{i_k}^X \mathbf{v}_{i_k}^X - w_{i_k}^X \right|^2 + (\mathbf{u}_{i_k}^X)^H \boldsymbol{\Sigma}_{i_k}^X \mathbf{u}_{i_k}^X}, \end{aligned} \quad (17)$$

where  $w_{i_k}^X$  is a complex weighting factor. By taking the derivative of  $\psi_{i_k}^X$  with respect to  $w_{i_k}^X$  and equating to zero, the optimal  $w_{i_k}^X$  maximizing  $\psi_{i_k}^X$  is given as

$$\tilde{w}_{i_k}^X = \frac{\left| (\mathbf{u}_{i_k}^X)^H \mathbf{H}_{i_k}^X \mathbf{v}_{i_k}^X \right|^2 + (\mathbf{u}_{i_k}^X)^H \boldsymbol{\Sigma}_{i_k}^X \mathbf{u}_{i_k}^X}{(\mathbf{v}_{i_k}^X)^H (\mathbf{H}_{i_k}^X)^H \mathbf{u}_{i_k}^X}. \quad (18)$$

Plugging (18) into (17), we obtain

$$\begin{aligned} \tilde{\psi}_{i_k}^X &= \frac{\left| (\mathbf{u}_{i_k}^X)^H \mathbf{H}_{i_k}^X \mathbf{v}_{i_k}^X \right|^2 + (\mathbf{u}_{i_k}^X)^H \boldsymbol{\Sigma}_{i_k}^X \mathbf{u}_{i_k}^X}{(\mathbf{u}_{i_k}^X)^H \boldsymbol{\Sigma}_{i_k}^X \mathbf{u}_{i_k}^X} \\ &= 1 + \gamma_{i_k}^X. \end{aligned} \quad (19)$$

From the relationship in (19), we can conclude that (14)-(16) is equivalent to (20)-(21) and achieve the same optimum point when  $w_{i_k}^X = \tilde{w}_{i_k}^X$ .

$$\begin{aligned} \max_{\mathbf{v}, \mathbf{u}, \mathbf{w}} \quad & \sum_{X \in \{UL, DL\}} \sum_{k=1}^K \sum_{i=1}^{I_k} \log_2 (\psi_{i_k}^X) \\ \text{s.t.} \quad & (15), (16), \end{aligned} \quad (20)$$

where  $\mathbf{w} = \{w_{i_k}^X : i_k \in \mathcal{I}, X \in \{UL, DL\}\}$  is the set of all weights. Note that (20)-(21) is easier to solve than (14)-(16), since only the denominator of  $\psi_{i_k}^X$  in (17) is a function of optimization variables  $\mathbf{v}_{i_k}^X$  and  $\mathbf{u}_{i_k}^X$ , but on the other hand both denominator and numerator of the  $\gamma_{i_k}^X$  in (11) are functions of the optimization variables. By plugging (17) into (20)-(21), we get

$$\begin{aligned} \max_{\mathbf{v}, \mathbf{u}, \mathbf{w}} \quad & \sum_{X \in \{UL, DL\}} \sum_{k=1}^K \sum_{i=1}^{I_k} \left( \log_2 (|w_{i_k}^X|^2) \right. \\ & \left. - \log_2 \left( \left| (\mathbf{u}_{i_k}^X)^H \mathbf{H}_{i_k}^X \mathbf{v}_{i_k}^X - w_{i_k}^X \right|^2 \right. \right. \\ & \left. \left. + (\mathbf{u}_{i_k}^X)^H \boldsymbol{\Sigma}_{i_k}^X \mathbf{u}_{i_k}^X \right) \right) \end{aligned} \quad (22)$$

$$\text{s.t.} \quad (15), (16). \quad (23)$$

Since (22)-(23) is not necessarily convex, we will introduce additional scaling factors  $t_{i_k}^X$  to reformulate (22)-(23) as a multi-convex optimization problem. With the new scaling

$$\begin{aligned} \boldsymbol{\Sigma}_{i_k}^{UL} &= \sum_{(l,j) \neq (i,k)} \mathbf{H}_{klj}^{UL} \mathbf{v}_{l_j}^{UL} (\mathbf{v}_{l_j}^{UL})^H (\mathbf{H}_{klj}^{UL})^H + \sum_{j=1}^K \sum_{l=1}^{I_j} \kappa \mathbf{H}_{klj}^{UL} \text{diag} \left( \mathbf{v}_{l_j}^{UL} (\mathbf{v}_{l_j}^{UL})^H \right) (\mathbf{H}_{klj}^{UL})^H \\ &+ \sum_{j=1, j \neq k}^K \sum_{l=1}^{I_j} \mathbf{H}_{kj}^{BB} \left( \mathbf{v}_{l_j}^{DL} (\mathbf{v}_{l_j}^{DL})^H + \kappa \text{diag} \left( \mathbf{v}_{l_j}^{DL} (\mathbf{v}_{l_j}^{DL})^H \right) \right) (\mathbf{H}_{kj}^{BB})^H \\ &+ \sum_{l=1}^{I_k} \mathbf{H}_k^{SI} \left( \mathbf{v}_{l_k}^{DL} (\mathbf{v}_{l_k}^{DL})^H + \kappa \text{diag} \left( \mathbf{v}_{l_k}^{DL} (\mathbf{v}_{l_k}^{DL})^H \right) \right) (\mathbf{H}_k^{SI})^H + \beta \sum_{j=1}^K \sum_{l=1}^{I_j} \text{diag} \left( \mathbf{H}_{klj}^{UL} \mathbf{v}_{l_j}^{UL} (\mathbf{v}_{l_j}^{UL})^H (\mathbf{H}_{klj}^{UL})^H \right) \\ &+ \beta \sum_{j=1, j \neq k}^K \sum_{l=1}^{I_j} \text{diag} \left( \mathbf{H}_{kj}^{BB} \mathbf{v}_{l_j}^{DL} (\mathbf{v}_{l_j}^{DL})^H (\mathbf{H}_{kj}^{BB})^H \right) + \beta \sum_{l=1}^{I_k} \text{diag} \left( \mathbf{H}_k^{SI} \mathbf{v}_{l_k}^{DL} (\mathbf{v}_{l_k}^{DL})^H (\mathbf{H}_k^{SI})^H \right) + \sigma_k^2 \mathbf{I}_{N_k}, \end{aligned} \quad (12)$$

$$\begin{aligned} \boldsymbol{\Sigma}_{i_k}^{DL} &= \sum_{(l,j) \neq (i,k)} \mathbf{H}_{ikj}^{DL} \mathbf{v}_{l_j}^{DL} (\mathbf{v}_{l_j}^{DL})^H (\mathbf{H}_{ikj}^{DL})^H + \sum_{j=1}^K \sum_{l=1}^{I_j} \kappa \mathbf{H}_{ikj}^{DL} \text{diag} \left( \mathbf{v}_{l_j}^{DL} (\mathbf{v}_{l_j}^{DL})^H \right) (\mathbf{H}_{ikj}^{DL})^H \\ &+ \sum_{(l,j) \neq (i,k)} \mathbf{H}_{ikl_j}^{UU} \left( \mathbf{v}_{l_j}^{UL} (\mathbf{v}_{l_j}^{UL})^H + \kappa \text{diag} \left( \mathbf{v}_{l_j}^{UL} (\mathbf{v}_{l_j}^{UL})^H \right) \right) (\mathbf{H}_{ikl_j}^{UU})^H \\ &+ \mathbf{H}_{i_k}^{SI} \left( \mathbf{v}_{i_k}^{UL} (\mathbf{v}_{i_k}^{UL})^H + \kappa \text{diag} \left( \mathbf{v}_{i_k}^{UL} (\mathbf{v}_{i_k}^{UL})^H \right) \right) (\mathbf{H}_{i_k}^{SI})^H + \beta \sum_{j=1}^K \sum_{l=1}^{I_j} \text{diag} \left( \mathbf{H}_{ikj}^{DL} \mathbf{v}_{l_j}^{DL} (\mathbf{v}_{l_j}^{DL})^H (\mathbf{H}_{ikj}^{DL})^H \right) \\ &+ \beta \sum_{(l,j) \neq (i,k)} \text{diag} \left( \mathbf{H}_{ikl_j}^{UU} \mathbf{v}_{l_j}^{UL} (\mathbf{v}_{l_j}^{UL})^H (\mathbf{H}_{ikl_j}^{UU})^H \right) + \beta \text{diag} \left( \mathbf{H}_{i_k}^{SI} \mathbf{v}_{i_k}^{UL} (\mathbf{v}_{i_k}^{UL})^H (\mathbf{H}_{i_k}^{SI})^H \right) + \sigma_{i_k}^2 \mathbf{I}_{N_{i_k}}. \end{aligned} \quad (13)$$

factors, we have

$$\max_{\mathbf{v}, \mathbf{u}, \mathbf{w}, \mathbf{t}} \sum_{X \in \{UL, DL\}} \sum_{k=1}^K \sum_{i=1}^{I_k} \left( \log_2 \left( |w_{i_k}^X|^2 \right) + \log_2 \left( t_{i_k}^X \right) - \frac{t_{i_k}^X}{\ln 2} \left( \left| (\mathbf{u}_{i_k}^X)^H \mathbf{H}_{i_k}^X \mathbf{v}_{i_k}^X - w_{i_k}^X \right|^2 + (\mathbf{u}_{i_k}^X)^H \boldsymbol{\Sigma}_{i_k}^X \mathbf{u}_{i_k}^X \right) \right) \quad (24)$$

$$\text{s.t.} \quad (15), (16), \quad (25)$$

which is a concave function of  $t_{i_k}^X$ , and  $\mathbf{t} = \{t_{i_k}^X : i_k \in \mathcal{I}, X \in \{UL, DL\}\}$  is the set of all scaling factors. To show the equivalence of (22)-(23) and (24)-(25), we first take the derivative of (24) with respect to  $t_{i_k}^X$  and then equate to zero. The optimum scaling factor is given as

$$\tilde{t}_{i_k}^X = \left( \left| (\mathbf{u}_{i_k}^X)^H \mathbf{H}_{i_k}^X \mathbf{v}_{i_k}^X - w_{i_k}^X \right|^2 + (\mathbf{u}_{i_k}^X)^H \boldsymbol{\Sigma}_{i_k}^X \mathbf{u}_{i_k}^X \right)^{-1}. \quad (26)$$

Substituting (26) into (24), we obtain (22). Therefore, we can conclude that under the optimum scaling factors  $\tilde{w}_{i_k}^X$  and  $\tilde{t}_{i_k}^X$ , the problem (24)-(25) is equivalent to (20)-(21).

Although the problem (24)-(25) is not jointly convex, it is component-wise convex. In other words, it is a convex function of one optimization variable when the other three optimization variables are fixed, which is known as multi-convex optimization problem [10]. The optimum scaling factors  $\tilde{w}_{i_k}^X$  and  $\tilde{t}_{i_k}^X$  can be computed from (18) and (26), respectively. The optimum receiving filters  $\mathbf{u}_{i_k}^X$  is expressed as

$$\tilde{\mathbf{u}}_{i_k}^X = \left( \mathbf{H}_{i_k}^X \mathbf{v}_{i_k}^X (\mathbf{v}_{i_k}^X)^H (\mathbf{H}_{i_k}^X)^H + \boldsymbol{\Sigma}_{i_k}^X \right)^{-1} \times (w_{i_k}^X)^H \mathbf{H}_{i_k}^X \mathbf{v}_{i_k}^X. \quad (27)$$

Under the fixed  $t_{i_k}^X$ ,  $w_{i_k}^X$  and  $\mathbf{u}_{i_k}^X$ , the problem (24)-(25) is a convex quadratically constrained quadratic problem, which can be solved using quadratic optimization tools [23]. The alternating iterative maximization algorithm is shown in Algorithm 1. Since a convex optimization problem is solved in each step of the algorithm, the objective function increases monotonically. Moreover, the objective function (24) is continuous and regular and the constraint sets of (25) are compact, and thus the algorithm is guaranteed to converge to a stationary point [24, Theorem 4.1(c)].

---

#### Algorithm 1 Sum-Rate Maximization Algorithm

---

- 1: Set the iteration number  $n = 0$  and initialize the transmit filters  $(\mathbf{v}_{i_k}^X)^{[0]}$  and scaling factors  $t_{i_k}^X$ ,  $w_{i_k}^X$ ,  $\forall (i, k, X)$ .
  - 2: **repeat**
  - 3:    $n \leftarrow n + 1$ .
  - 4:   Update the receive filter  $(\mathbf{u}_{i_k}^X)^{[n]}$ ,  $\forall (i, k, X)$  using (27).
  - 5:   Calculate the transmit filter  $(\mathbf{v}_{i_k}^X)^{[n]}$ ,  $\forall (i, k, X)$  by solving (24)-(25) using quadratic optimization tools.
  - 6:   Update the scaling factor  $(t_{i_k}^X)^{[n]}$ ,  $\forall (i, k, X)$  using (26).
  - 7:   Update the scaling factor  $(w_{i_k}^X)^{[n]}$ ,  $\forall (i, k, X)$  using (18).
  - 8: **until** convergence or maximum number of iterations is reached.
- 

Similar to prior work dealing with beamforming and interference management, we assume that perfect channel-state-information (CSI) knowledge is available at the BSs. Channels between BSs and users can be estimated using standard 3GPP LTE channel estimation protocols for HD systems. Channels between the users can be learned via neighbour discovery methods applicable to device-to-device (D2D) communication, such as sounding reference signals (SRS) in 3GPP LTE [25].

#### B. Sum Rate Maximization With QoS Constraints

As we will see in the simulations, the sum-rate maximization problem without QoS constraints can result in unfair allocation of resources, and some users in bad channel conditions are not served. Therefore, in this subsection, we consider the sum rate maximization problem subject to both power and QoS constraints. The problem is formulated as

$$\max_{\mathbf{v}, \mathbf{u}} \sum_{X \in \{UL, DL\}} \sum_{k=1}^K \sum_{i=1}^{I_k} \log_2 (1 + \gamma_{i_k}^X) \quad (28)$$

$$\text{s.t.} \quad (\mathbf{v}_{i_k}^{UL})^H \mathbf{v}_{i_k}^{UL} \leq P_{i_k}, \quad i_k \in \mathcal{I}, \quad (29)$$

$$\sum_{i=1}^{I_k} (\mathbf{v}_{i_k}^{DL})^H \mathbf{v}_{i_k}^{DL} \leq P_k, \quad k \in \mathcal{K}, \quad (30)$$

$$\log_2 (1 + \gamma_{i_k}^X) \geq R_{i_k}^X, \quad i_k \in \mathcal{I}, \quad X \in \{UL, DL\} \quad (31)$$

where  $R_{i_k}^X$  is the data rate threshold for user  $i_k \in \mathcal{I}$  in the  $X$  channel,  $X \in \{UL, DL\}$ .

The optimal receive beamforming vector for the problem (28)-(31) is the MMSE receiver given as

$$\tilde{\mathbf{u}}_{i_k}^X = \left( \mathbf{H}_{i_k}^X \mathbf{v}_{i_k}^X (\mathbf{v}_{i_k}^X)^H (\mathbf{H}_{i_k}^X)^H + \boldsymbol{\Sigma}_{i_k}^X \right)^{-1} \mathbf{H}_{i_k}^X \mathbf{v}_{i_k}^X. \quad (32)$$

It is well-known that when receivers apply the MMSE receive beamformers, the mean-squared-error (MSE) and SINR are related as [26].

$$(\text{MSE}_{i_k}^X)^{-1} = 1 + \gamma_{i_k}^X, \quad (33)$$

where  $\text{MSE}_{i_k}^X$  can be computed as

$$\text{MSE}_{i_k}^X = \left| (\mathbf{u}_{i_k}^X)^H \mathbf{H}_{i_k}^X \mathbf{v}_{i_k}^X - 1 \right|^2 + (\mathbf{u}_{i_k}^X)^H \boldsymbol{\Sigma}_{i_k}^X \mathbf{u}_{i_k}^X. \quad (34)$$

By applying (33), we can reformulate (28)-(31) as the following sum log-MSE maximization problem

$$\max_{\mathbf{v}, \mathbf{u}} \sum_{X \in \{UL, DL\}} \sum_{k=1}^K \sum_{i=1}^{I_k} \log_2 \left( (\text{MSE}_{i_k}^X)^{-1} \right) \quad (35)$$

$$\text{s.t.} \quad (29), (30), \quad (36)$$

$$\log_2 \left( (\text{MSE}_{i_k}^X)^{-1} \right) \geq R_{i_k}^X, \quad \forall (i, k, X). \quad (37)$$

We follow the successive convex approximation (SCA) approach proposed in [16] to relax (35)-(37) by introducing MSE upper bounds with a monotonic log-concave function, i.e.,  $\text{MSE}_{i_k}^X \leq g(t_{i_k}^X)^{-1}$ , where  $t_{i_k}^X$  is an auxiliary variable. Assuming  $g(t_{i_k}^X)$  as  $g(t_{i_k}^X) = 2^{-t_{i_k}^X}$ , which is shown to

perform well [16], the equivalent optimization problem is formulated as

$$\min_{\mathbf{v}, \mathbf{u}, \mathbf{t}} \sum_{X \in \{UL, DL\}} \sum_{k=1}^K \sum_{i=1}^{I_k} t_{i_k}^X \quad (38)$$

$$\text{s.t.} \quad (29), (30), \quad (39)$$

$$-t_{i_k}^X \geq R_{i_k}^X, \quad i_k \in \mathcal{I}, \quad X \in \{UL, DL\}, \quad (40)$$

$$\text{MSE}_{i_k}^X \leq 2^{t_{i_k}^X}, \quad i_k \in \mathcal{I}, \quad X \in \{UL, DL\}. \quad (41)$$

Since the problem (38)-(41) is still non-convex, we approximate the non-convex parts of the MSE constraints (41) with the first-order Taylor series approximation iteratively. Applying this approximation, at the  $n$ th iteration we have

$$\min_{\mathbf{v}, \mathbf{u}, \mathbf{t}} \sum_{X \in \{UL, DL\}} \sum_{k=1}^K \sum_{i=1}^{I_k} t_{i_k}^X \quad (42)$$

$$\text{s.t.} \quad (29), (30), \quad (43)$$

$$-t_{i_k}^X \geq R_{i_k}^X, \quad i_k \in \mathcal{I}, \quad X \in \{UL, DL\}, \quad (44)$$

$$\begin{aligned} \text{MSE}_{i_k}^X &\leq \ln(2) 2^{(t_{i_k}^X)^{[n]}} t_{i_k}^X \\ &\quad + 2^{(t_{i_k}^X)^{[n]}} \left( 1 - \ln(2) 2^{(t_{i_k}^X)^{[n]}} \right), \\ &\quad i_k \in \mathcal{I}, \quad X \in \{UL, DL\}. \end{aligned} \quad (45)$$

Although the problem (42)-(45) is convex under the fixed receiver beamforming vectors, the constraint set is highly complex, and the user rate constraints impose feasibility issues that are difficult to manage. To this end, we simplify the constraint set by Lagrangian relaxation of the rate constraints [16], and the relaxed problem is given as

$$\min_{\mathbf{v}, \mathbf{u}, \mathbf{t}} \sum_{X \in \{UL, DL\}} \sum_{k=1}^K \sum_{i=1}^{I_k} (t_{i_k}^X + \lambda_{i_k}^X (R_{i_k}^X + t_{i_k}^X)) \quad (46)$$

$$\text{s.t.} \quad (29), (30), \quad (47)$$

$$\begin{aligned} \text{MSE}_{i_k}^X &\leq \ln(2) 2^{(t_{i_k}^X)^{[n]}} t_{i_k}^X \\ &\quad + 2^{(t_{i_k}^X)^{[n]}} \left( 1 - \ln(2) 2^{(t_{i_k}^X)^{[n]}} \right), \\ &\quad i_k \in \mathcal{I}, \quad X \in \{UL, DL\}. \end{aligned} \quad (48)$$

From the KKT conditions of the problem (46)-(48), we can solve the dual variables  $\alpha_{i_k}^X$  corresponding to the MSE constraints (48) as

$$(\alpha_{i_k}^X)^{[n+1]} = \frac{1 + (\lambda_{i_k}^X)^{[n]}}{\ln(2) 2^{(t_{i_k}^X)^{[n]}}}, \quad i_k \in \mathcal{I}, \quad X \in \{UL, DL\}. \quad (49)$$

The auxiliary variable  $(t_{i_k}^X)^{[n+1]}$  can be updated using the complementary slackness constraint, and the update is expressed as

$$(t_{i_k}^X)^{[n+1]} = \frac{\text{MSE}_{i_k}^X - \left( 2^{(t_{i_k}^X)^{[n]}} \left( 1 - \ln(2) 2^{(t_{i_k}^X)^{[n]}} \right) \right)}{\ln(2) 2^{(t_{i_k}^X)^{[n]}}}. \quad (50)$$

Moreover, from the KKT conditions, the optimal transmit beamforming vectors are written as

$$\tilde{\mathbf{v}}_{i_k}^X = \alpha_{i_k}^X \left( \mathbf{X}_{i_k}^X(\mathbf{u}) + \bar{\tau}_{i_k}^X \mathbf{I}_{M_{i_k}^X} \right)^{-1} (\mathbf{H}_{i_k}^X)^H \mathbf{u}_{i_k}^X, \quad (51)$$

where  $\mathbf{X}_{i_k}^X(\mathbf{u})$  is defined in (52)-(53),  $\bar{\tau}_{i_k}^X$ , the dual variable for the power constraints is given at the bottom of the following page in (54).

In the dual update, the rate weight factors  $\lambda_{i_k}^X$  are updated from the violation of the rate constraints using subgradient method as

$$(\lambda_{i_k}^X)^{[n+1]} = \left( (\lambda_{i_k}^X)^{[n]} + (\mu_{i_k}^X)^{[n]} \left( R_{i_k}^X + (t_{i_k}^X)^{[n]} \right) \right)^+, \quad (55)$$

where  $(\mu_{i_k}^X)^{[n]}$  is the step size at the  $n$ th iteration. The steps of the algorithm are shown in Algorithm 2.

---

**Algorithm 2** Sum-Rate Maximization Algorithm with QoS Constraints

---

- 1: Initialize the transmit filters  $(\mathbf{v}_{i_k}^X)^{[0]}$  and auxiliary variables  $(t_{i_k}^X)^{[0]}$  and rate weights  $(\lambda_{i_k}^X)^{[0]} = 0$ ,  $i_k \in \mathcal{I}$ ,  $X \in \{UL, DL\}$ .
  - 2: **repeat**
  - 3:     Update the receive filter  $\mathbf{u}_{i_k}^X$ ,  $\forall (i, k, X)$  using (32).
  - 4:      $n = 1$ .
  - 5:     **repeat**
  - 6:         Update the rate weights  $(\lambda_{i_k}^X)^{[n]}$ ,  $\forall (i, k, X)$  using (55).
  - 7:         Update the dual variables  $(\alpha_{i_k}^X)^{[n]}$ ,  $\forall (i, k, X)$  using (49).
  - 8:         Calculate the transmit filter  $\tilde{\mathbf{v}}_{i_k}^X$ ,  $\forall (i, k, X)$  from (51).
  - 9:         Update the auxiliary variables  $(t_{i_k}^X)^{[n]}$ ,  $\forall (i, k, X)$  using (50).
  - 10:         $n \leftarrow n + 1$ .
  - 11:     **until** convergence or maximum number of iterations is reached.
  - 12: **until** convergence or maximum number of iterations is reached.
- 

Note that the problem (28)-(31) can be inherently infeasible under tight power and high QoS constraints. However, even in this case the algorithm can find a region, where the QoS constraint violation is reasonably small.

### III. SIMULATION RESULTS

In this section, we numerically investigate the sum-rate maximization problem in both single and multi-cell MIMO FD multi-user systems. We compare the proposed algorithm with the HD algorithm under the 3GPP LTE specifications for small cell deployments [27]. We consider small cells, since small cells are considered to be suitable for deployment of FD technology due to low transmit powers, short transmission distances and low mobility [6], [28], [29]. Note that although we have presented the most general scenario, i.e. FD BSs and FD users, in the next generation wireless communication systems, the users are still envisioned to be operating in HD mode. Therefore, in our simulations, we assume HD users.

### A. Single-Cell

A single hexagonal cell having a BS in the center with  $M_0 = 4$  transmit and  $N_0 = 4$  receive antennas with randomly distributed  $K = 2$  UL and  $J = 2$  DL users equipped with 2 antennas is simulated<sup>1</sup>.

The channel between BS and users are assumed to experience the path loss model for line-of-sight (LOS) and non-line-of-sight (NLOS) communications depending on the probability

$$P_{\text{LOS}} = 0.5 - \min(0.5, 5 \exp(-0.156/d)) + \min(0.5, 5 \exp(-d/0.03)), \quad (56)$$

where  $d$  is the distance between BS and users in km. Detailed simulation parameters are shown in Table I.

The channel gain between the BS to  $k$ th UL user is given by  $\mathbf{H}_k^{UL} = \sqrt{\kappa_k^{UL}} \tilde{\mathbf{H}}_k^{UL}$ , where  $\tilde{\mathbf{H}}_k^{UL}$  denotes the small scale fading following a complex Gaussian distribution with zero mean and unit variance, and  $\kappa_k^{UL} = 10^{(-X/10)}$ ,  $X \in \{\text{LOS}, \text{NLOS}\}$  represents the large scale fading consisting of path loss and shadowing, where LOS and NLOS are calculated from a specific path loss model given in Table I. The channel between BS and DL users is defined similarly. The channel between UL and DL users, i.e., CCI channel, is given by  $\mathbf{H}_{jk}^{DU} = \sqrt{\epsilon} \sqrt{\kappa_{jk}^{DU}} \tilde{\mathbf{H}}_{jk}^{DU}$  where  $\tilde{\mathbf{H}}_{jk}^{DU}$  and  $\kappa_{jk}^{DU}$  represent the same concept as  $\tilde{\mathbf{H}}_k^{UL}$  and  $\kappa_k^{UL}$ , respectively. The factor  $\epsilon$  represents the obtained isolation among the UL and DL users,

<sup>1</sup>Note that although the BS has  $N_0 + M_0$  antennas in total, similar to [8], we assume that only  $M_0$  ( $N_0$ ) antennas can be used for transmission (reception) in HD mode. This is because in practical systems RF front-ends (e.g. ADC/DAC, mixers, filters, etc.) are much more expensive than antennas and therefore are more scarce resources. Therefore, we assume that BS only has  $M_0$  transmission front-ends and  $N_0$  receiving front-ends.

TABLE I. SIMULATION PARAMETERS FOR SINGLE-CELL

Parameter	Settings
Cell Radius	40m
Carrier Frequency	2GHz
Maximum BS Power	24dBm
Maximum UL user Power	23dBm
Bandwidth	10MHz
Thermal Noise Density	-174dBm/Hz
Noise Figure	BS: 13dB, User: 9dB
Path Loss (dB) between BS and users ( $d$ in km)	LOS: $103.8 + 20.9 \log_{10} d$ NLOS: $145.4 + 37.5 \log_{10} d$
Path Loss (dB) between users ( $d$ in km)	LOS: $98.45 + 20 \log_{10} d$ , $d \leq 50\text{m}$ NLOS: $175.78 + 40 \log_{10} d$ , $d > 50\text{m}$
Shadowing Standard Deviation	LOS: 3dB, NLOS: 4dB

via a channel assignment phase that determines which users would coexist on the same channel, please see Subsection III-B for elaboration. For the self-interference channel, we adopt the model in [1], in which the self-interference channel is distributed as  $\mathbf{H}_0 \sim \mathcal{CN}\left(\sqrt{\frac{K_R}{1+K_R}} \tilde{\mathbf{H}}_0, \frac{1}{1+K_R} \mathbf{I}_{N_0} \otimes \mathbf{I}_{M_0}\right)$ , where  $K_R$  is the Rician factor,  $\tilde{\mathbf{H}}_0$  is a deterministic matrix<sup>2</sup>.

In Fig. 2 and Fig. 3 the resulting spectral efficiency of the network, via the utilization of the proposed design, is numerically evaluated and compared to the HD counterpart. In particular, the legends 'FD', 'FD-UL', 'FD-DL', represent the network sum rate in the proposed FD system, and portions of the network sum rate realized in UL and DL paths, respectively. The legends 'HD', 'HD-UL', 'HD-DL', present

<sup>2</sup>Similar to [6], without loss of generality, we set  $K_R = 1$  and  $\tilde{\mathbf{H}}_0$  to be the matrix of all ones for all experiments.

$$\begin{aligned} \mathbf{X}_{i_k}^{UL}(\mathbf{u}) &= \sum_{j=1}^K \sum_{l=1}^{I_j} \alpha_{l_j}^{UL} \left( (\mathbf{H}_{j i_k}^{UL})^H \mathbf{u}_{l_j}^{UL} (\mathbf{u}_{l_j}^{UL})^H \mathbf{H}_{j i_k}^{UL} + \beta (\mathbf{H}_{j i_k}^{UL})^H \text{diag} \left( \mathbf{u}_{l_j}^{UL} (\mathbf{u}_{l_j}^{UL})^H \right) \mathbf{H}_{j i_k}^{UL} \right) \\ &+ \alpha_{i_k}^{DL} \kappa \text{diag} \left( (\mathbf{H}_{i_k}^{SI})^H \mathbf{u}_{i_k}^{DL} (\mathbf{u}_{i_k}^{DL})^H \mathbf{H}_{i_k}^{SI} \right) + \alpha_{i_k}^{DL} \beta (\mathbf{H}_{i_k}^{SI})^H \text{diag} \left( \mathbf{u}_{i_k}^{DL} (\mathbf{u}_{i_k}^{DL})^H \right) \mathbf{H}_{i_k}^{SI} \\ &+ \sum_{(l,j) \neq (i,k)} \alpha_{l_j}^{DL} \left( (\mathbf{H}_{l_j i_k}^{UU})^H \mathbf{u}_{l_j}^{DL} (\mathbf{u}_{l_j}^{DL})^H \mathbf{H}_{l_j i_k}^{UU} + \beta (\mathbf{H}_{l_j i_k}^{UU})^H \text{diag} \left( \mathbf{u}_{l_j}^{DL} (\mathbf{u}_{l_j}^{DL})^H \right) \mathbf{H}_{l_j i_k}^{UU} \right), \quad (52) \end{aligned}$$

$$\begin{aligned} \mathbf{X}_{i_k}^{DL}(\mathbf{u}) &= \sum_{j=1, j \neq k}^K \sum_{l=1}^{I_j} \alpha_{l_j}^{UL} \left( (\mathbf{H}_{j k}^{BB})^H \mathbf{u}_{l_j}^{UL} (\mathbf{u}_{l_j}^{UL})^H \mathbf{H}_{j k}^{BB} + \beta (\mathbf{H}_{j k}^{BB})^H \text{diag} \left( \mathbf{u}_{l_j}^{UL} (\mathbf{u}_{l_j}^{UL})^H \right) \mathbf{H}_{j k}^{BB} \right) \\ &+ \sum_{l=1}^{I_k} \alpha_{l_k}^{UL} \left( \kappa \text{diag} \left( (\mathbf{H}_k^{SI})^H \mathbf{u}_{l_k}^{UL} (\mathbf{u}_{l_k}^{UL})^H \mathbf{H}_k^{SI} \right) + \beta (\mathbf{H}_k^{SI})^H \text{diag} \left( \mathbf{u}_{l_k}^{UL} (\mathbf{u}_{l_k}^{UL})^H \right) \mathbf{H}_k^{SI} \right) \\ &+ \sum_{j=1}^K \sum_{l=1}^{I_j} \alpha_{l_j}^{DL} \left( (\mathbf{H}_{l_j k}^{DL})^H \mathbf{u}_{l_j}^{DL} (\mathbf{u}_{l_j}^{DL})^H \mathbf{H}_{l_j k}^{DL} + \beta (\mathbf{H}_{l_j k}^{DL})^H \text{diag} \left( \mathbf{u}_{l_j}^{DL} (\mathbf{u}_{l_j}^{DL})^H \right) \mathbf{H}_{l_j k}^{DL} \right). \quad (53) \end{aligned}$$

$$(\bar{\tau}_{i_k}^X, \bar{M}_{i_k}^X) = \begin{cases} (\tau_{i_k}, M_{i_k}) & \text{if } X = UL, \\ (\tau_k, M_k) & \text{if } X = DL. \end{cases} \quad (54)$$

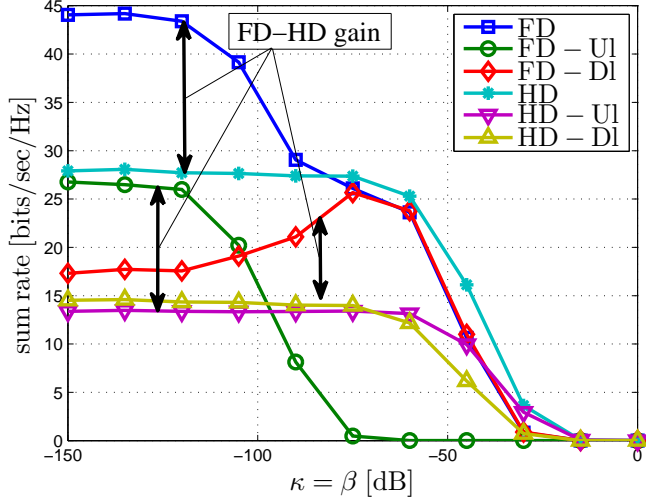


Fig. 2. Network spectral efficiency [bits/sec/Hz] vs. transceiver operational accuracy  $\kappa = \beta$  [dB]. A significant gain is observed via the application of the proposed FD scheme, for an accurate operation of the FD transceivers.

the same meaning for a system with HD operation at the BS. In each case, the evaluated sum-rate, in terms of [bits/sec/Hz], is averaged over more than 100 channel realizations.

Unless otherwise is stated, the following values are used in the default simulation setup:  $\kappa = \beta = -120$ dB,  $p_0 = 30$ dBm,  $\epsilon = -20$ dB,  $K = 2$  UL users,  $J = 2$  DL users,  $M_0 = N_0 = 4$  transmit and receive antennas at the BS,  $N_j = 2$  receive antennas at DL users,  $M_k = 2$  transmit antennas at UL users.

In Fig. 2, the resulting network sum rate is illustrated, for different levels of the transceiver accuracy. It is observed that a higher accuracy results in a higher gain for the FD scheme, as it results in a better self-interference cancellation, see (5), (7). In this respect, the quality of the HD scheme is more robust compared to a FD system, due to the absence of the strong self-interference path.

Moreover, it is observed that for a FD system with high transceiver accuracy, the UL communication holds a higher quality, compared to DL. This is grounded on the effect of CCI, which reduces the quality of DL transmission, compared to UL. On the other hand, as the transceiver accuracy decreases, the FD scheme tends to allocate more resources on the DL path and drastically reduces the UL resources, in order to obtain a higher overall sum-rate. This is perceivable since the UL communication is suffered from the effect of inaccurate self-interference cancellation. Please note that such fluctuations occurs with much less intensity for a HD system, where UL and DL communications obtain a relatively equal average rate, at the optimality.

In Fig. 3, the impact of the affordable transmit power is illustrated on the resulting network spectral efficiency. As expected, it is observed that a higher affordable transmit power results in a higher spectral efficiency, for both FD and HD schemes. Similar to Fig. 2, it is observed that the DL and UL

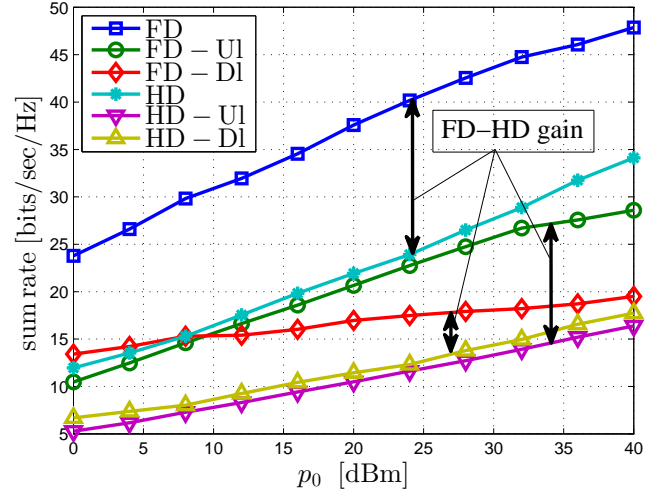


Fig. 3. Network spectral efficiency [bits/sec/Hz] vs. transmit power constraints  $p_0$  [dBm]. A higher affordable transmit power results in a higher spectral efficiency, for both FD and HD schemes.

communications obtain a relatively similar average share of sum rate in a HD setup. On the other hand, for a relatively accurate FD transceiver (simulated in Fig. 3), as the transmit power level increases the network performance is dominated by the effect of CCI paths. This results in a larger preference of the UL communication paths over the DL, which are degraded due to the effect of CCI.

TABLE II. SIMULATION PARAMETERS FOR MULTI-CELL

Parameter	Settings
Cell Radius	40m
Minimum Distance between BSs	40m
Carrier Frequency	2GHz
Bandwidth	10MHz
Thermal Noise Density	-174dBm/Hz
Noise Figure	BS: 13dB, User: 9dB
Path Loss (dB) between BS and users ( $d$ in km)	LOS: $103.8 + 20.9 \log_{10} d$ NLOS: $145.4 + 37.5 \log_{10} d$
Path Loss (dB) between users ( $d$ in km)	$98.45 + 20 \log_{10} d, d \leq 50m$ $175.78 + 40 \log_{10} d, d > 50m$
Path Loss (dB) between BSs ( $d$ in km)	LOS: $89.5 + 16.9 \log_{10} d, d < 2/3km,$ LOS: $101.9 + 40 \log_{10} d, d \geq 2/3km,$ NLOS: $169.36 + 40 \log_{10} d$
Shadowing Standard Deviation between BS and users	LOS: 3dB, NLOS: 4dB
Shadowing Standard Deviation between BSs	6dB

### B. Multi-Cell

In this section, we consider an outdoor multi-cell scenario with eight Pico cells randomly dropped in an area of a hexagonal cell with height of 500 meters. For brevity, we set the same number of transmit and receive antennas at each BS, i.e.  $M_k = N_k = N, k \in \mathcal{K}$ , and at each user i.e.  $M_{i_k} = N_{i_k} = M, i_k \in \mathcal{I}$ . The BSs are assumed to have  $N = 4$  transmit and receive antennas, and randomly distributed 10 users in each cell, i.e., 5 UL and 5 DL HD users, are equipped with  $M = 2$  transmit and receive antennas. The probability of LOS for the channel between BSs, and BSs and users is computed from (56). Detailed simulation parameters are shown in the Table II.

In Figs. 4, 5 and 6, the resulting spectral efficiency of the network, via the utilization of the proposed design is numerically evaluated and compared to the HD counterpart. The used legends present the same meaning as for Subsection III-A, where the sum rate is calculated as the collective communication rate [bits/sec/Hz] over all links, and all cells. In each case, the evaluated sum-rate is averaged over more than 100 channel realizations. Unless otherwise is stated, the defined values in Subsection III-A are used as the default network parameters.

In Fig. 4, the resulting network sum rate is illustrated, for different levels of the transceiver accuracy. Similar to Fig. 2, it is observed that a higher accuracy results in a higher gain for the FD scheme where the quality of the HD scheme is observed to be more robust compared to a FD system. Moreover, as it is observed from Fig. 2, while the majority of the network resources are allocated to the UL communication paths for a system with high transceiver accuracy, this paradigm is reversed as  $\kappa$  and  $\beta$  increase. The reason is that the UL communication paths are suffered from the residual self-interference as the transceiver accuracy decrease.

In Fig. 5, the impact of the affordable transmit power is

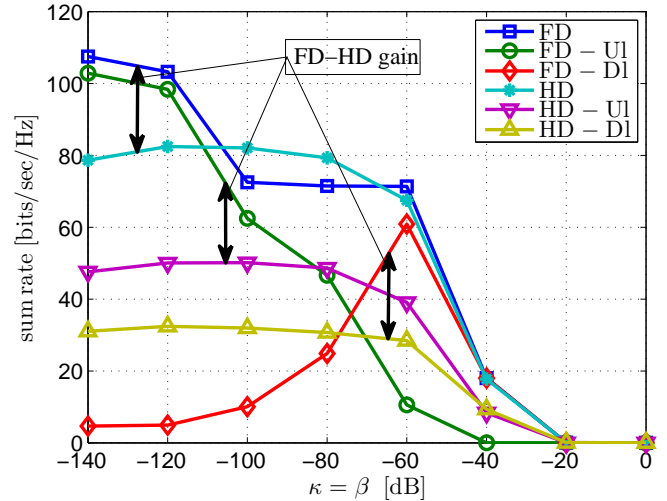


Fig. 4. Network spectral efficiency [bits/sec/Hz] vs. transceiver operational accuracy  $\kappa = \beta$  [dB]. The gainful application of FD scheme is observed for an accurate operation of the FD transceivers.

illustrated on the resulting network spectral efficiency, for two levels of the transceiver accuracy, i.e.,  $\kappa = \beta = -100$  [dB], and  $\kappa = \beta = -150$  [dB]. As expected, it is observed that a higher affordable transmit power results in a higher spectral efficiency, for both FD and HD schemes, and for both simulated levels of  $\kappa$ . Furthermore, it is observed that the scenario with a higher transceiver accuracy obtains a higher overall sum rate. Nevertheless, the obtained rate for the DL communication paths are smaller with a higher transceiver accuracy. This is a similar observation as in Fig. 4, where the DL capacity obtains a dominant role with a big  $\kappa$ , and receives a larger portion of the network resources, as the UL paths are largely degraded due to the effect of self-interference.

It is observed that a gainful application of FD operation at the BS is largely dependent on the smart control of the interference paths, which additionally appear in a FD network, see Section II. In this paper, we have discussed the role of optimal transmit strategy design, with the goal of maximizing the network sum rate, given a set of randomly positioned users sharing the same channel. It is known that in a realistic system, a network scheduler decides on the sub-set of the users which shall coexist at the same channel, i.e., via a channel assignment process [30]<sup>3</sup>. This is, in particular, a practical way to reduce the destructive CCI interference paths which appear in a FD system, e.g., users with with strong CCI shall be assigned to different channels.

In order to incorporate the effect of a successful channel assignment phase in the simulated network sum rate, we introduce a CCI isolation factor  $\epsilon$ , which scales down the intensity of the CCI channel in the network. In this respect  $\epsilon = 1$  represents the scenario with no channel assignment

<sup>3</sup>In our setup, the channel assignment phase can be interpreted as separating the users into different operating frequency bands.

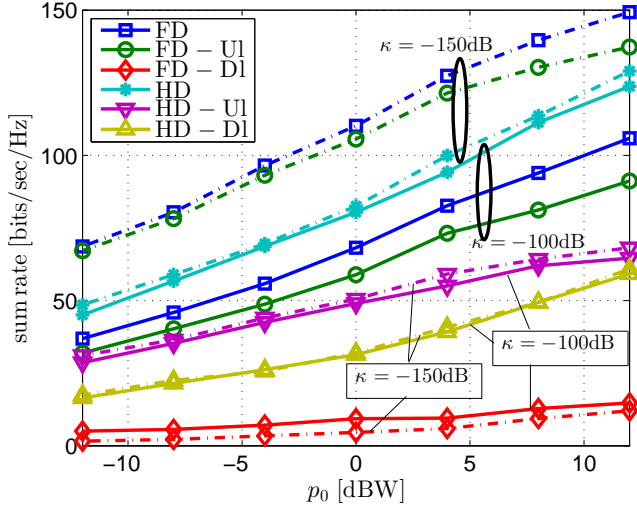


Fig. 5. Network spectral efficiency [bits/sec/Hz] vs. allowed transmit power [dBW]. Different levels of transceiver accuracy is simulated ( $\kappa = \beta$  [dB]). The solid (dashed) lines represent the case with lower (higher) transceiver accuracy, i.e.,  $\kappa = -100$  [dB] ( $\kappa = -150$  [dB]). A higher affordable transmit power results in a higher spectral efficiency, for both FD and HD schemes.

phase, and hence no reduction in the strength of CCI, while  $\epsilon = 0$  represents a perfect CCI reduction, which is not achievable in practice.

In Fig. 6, the impact of  $\epsilon$  is observed on the resulting network sum rate. As expected, the performance of the HD setup does not depend on the value of  $\epsilon$ , as the CCI channel does not exist for a HD setup. On the other hand, the FD setup achieves a higher spectral efficiency, as the UL-DL isolation is enhanced. In particular, for the simulated setup in Fig. 6, it is shown that a successful isolation of the UL/DL paths result in an effective improvement of the network performance, where a strong CCI results in a lower network sum rate, in comparison to the HD counterpart.

### C. Multi-Convex vs. WMMSE Optimization

Similar to the WMMSE method, see [8], the proposed multi-convex design method in Subsection II-A provides an iterative convex optimization framework. In general, due to the jointly non-convex nature of the resulting problem, the global optimality of the obtained optimum point can not be guaranteed. In this respect, the proposed multi-convex method leads to the decomposition of the original problem into a larger variable domain, which may become favorable in dealing with local optimal points, see Subsection II-A for more elaboration. In Fig. 7 it is observed that the proposed multi-convex optimization method ('MultiCVX') is capable of adding a marginal gain to that of the WMMSE ('WMMSE') method. Moreover, it is observed that the aforementioned gain is achievable for a high transceiver accuracy, i.e., lower  $\kappa, \beta$  where for a larger values of  $\kappa$  and  $\beta$  the aforementioned gain disappears. This is perceivable, as for the higher value of transceiver inaccuracy,

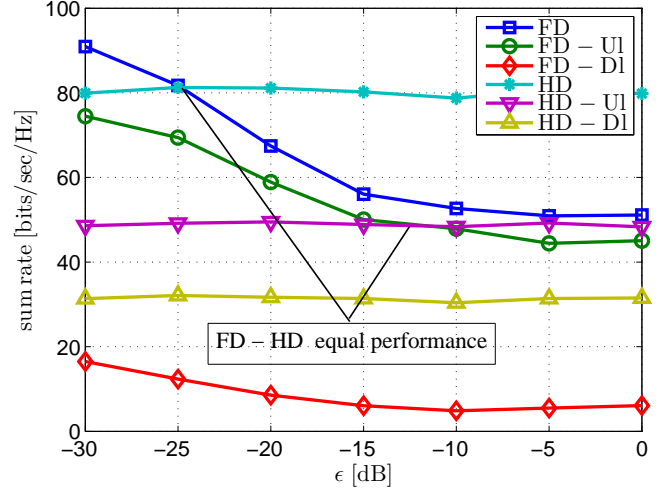


Fig. 6. Network spectral efficiency [bits/sec/Hz] vs. CCI reduction factor  $\epsilon$  [dB]. CCI intensity impacts, destructively, the performance of the FD setup.  $\kappa = \beta = -100$  [dB].

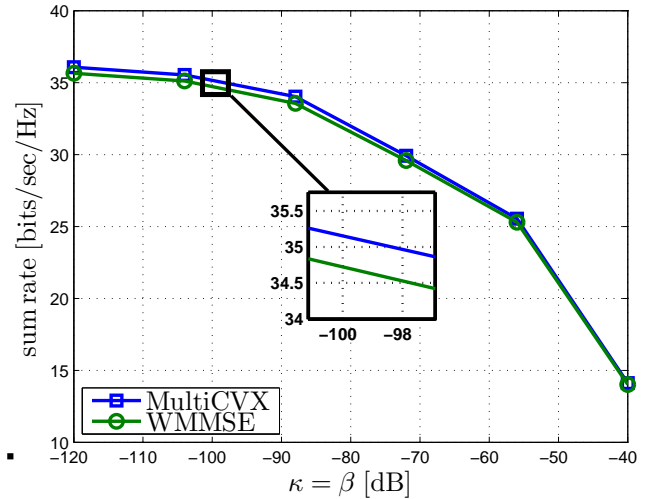


Fig. 7. Network spectral efficiency [bits/sec/Hz] vs. transceiver operational accuracy  $\kappa = \beta$  [dB]. The proposed Multi-Convex optimization improves the obtained performance by the weighted minimum-mean-squared error (WMMSE) method. See Subsection III-A for the used parameter setting.

only one of the UL and DL paths may be active due to the strong effect of self-interference. This results in a simplified solution structure and effectively eliminates the possibility of a local optimum points. It is worth mentioning, according to the performed simulations, both multi-convex and WMMSE methods result in a closely similar number of the optimization iterations, and consequently result in a similar computational complexity.

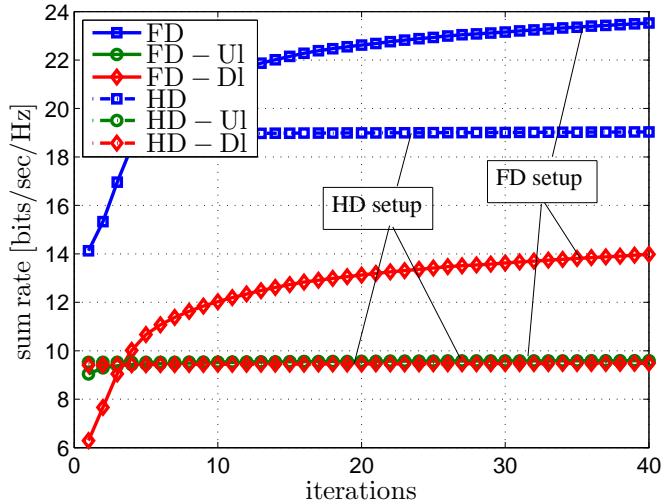


Fig. 8. Network spectral efficiency [bits/sec/Hz] vs. optimization iteration count. The strictly monotonic (increasing) nature of the sum rate is observable as the iteration count increases.

#### D. Convergence

As it is elaborated in Subsection II-A, the proposed multi-convex optimization is based on the iterative update of the design parameters, until a stable, i.e., a local optimal solution, is obtained. Hence, it is of our interest to observe how the design iterations impact the resulting sum rate. In Fig. 8, the resulting network sum rate is observed, over multiple design iterations. This is obtained by averaging the convergence behavior of the network, over the several simulated values of  $\kappa, \beta$  in Fig. 2. As expected, the strictly increasing behavior of the optimization objective is observed as the number of iterations increases. Moreover, it is observed that the HD setup converges with relatively smaller number of the optimization iterations, compared to the FD counterpart. This is perceivable, as the design of a FD setup needs to manage further considerations regarding the self-interference and CCI paths, which result in a relatively slower design process.

#### IV. CONCLUSION

In this work, we have addressed the transmit and receive filter design for sum-rate maximization problem in an FD MIMO multi-cell system with FD users. Both self-interference and CCI in the system under the limited DR at the transmitters and receivers are taken into account. Since the globally optimal solution is difficult to obtain due to the non-convex nature of the problem, an alternating iterative algorithm to find a stationary optimum is proposed based on the reformulation of the optimization problem as a multi-convex optimization problem. As an extension, we have provided a solution for the sum-rate maximization problem under QoS constraints, where each user has to achieve a data rate constraint. It is shown in simulations that the sum-rate achieved by FD mode is higher than the sum-rate achieved by baseline HD

schemes at moderate interference levels, but its performance is outperformed by baseline schemes at high interference levels.

#### REFERENCES

- [1] M. Duarte, C. Dick, and A. Sabharwal, "Experiment-driven characterization of full-duplex wireless systems," *IEEE Trans. Wireless Commun.*, vol. 11, no. 12, pp. 4296-4307, Dec. 2012.
- [2] Y. Hua, P. Liang, Y. Ma, A. C. Cirik and Q. Gao, "A method for broadband full-duplex MIMO radio," *IEEE Signal Process. Lett.*, vol. 19, no. 12, pp. 793-796, Dec 2012.
- [3] D. Bharadia and S. Katti, "Full duplex MIMO radios," in *Proc. 11th USENIX Conf. on Networked Systems Design and Implementation (NSDI)*, pp. 359-372, April 2014.
- [4] Y. Hua, Y. Ma, A. Gholian, Y. Li, A. C. Cirik, P. Liang, "Radio self-interference cancellation by transmit beamforming, all-analog cancellation and blind digital tuning," *Elsevier Signal Process.*, vol. 108, pp. 322-340, March 2015.
- [5] D. Kim, H. Lee, and D. Hong, "A Survey of in-band full-duplex transmission: From the perspective of PHY and MAC layers," *IEEE Communications Surveys & Tutorials*, vol. 17, no. 4, pp. 2017-2046, Fourth quarter 2015.
- [6] D. Nguyen, L. Tran, P. Pirinen, and M. Latva-aho, "On the spectral efficiency of full-duplex small cell wireless systems," *IEEE Trans. Wireless Commun.*, vol. 13, no. 9, pp. 4896-4910, Sept. 2014.
- [7] S. Huberman, and T. Le-Ngoc, "MIMO full-duplex precoding: A joint beamforming and self-interference cancellation structure," *IEEE Trans. Wireless Commun.*, vol. 14, no. 4, pp. 2205-2217, Apr. 2015.
- [8] S. Li, R. Murch, and V. Lau, "Linear transceiver design for full-duplex multi-user MIMO system," *IEEE Int. Conf. Commun. (ICC)*, pp. 4921-4926, June 2014.
- [9] B. P. Day, A. R. Margetts, D. W. Bliss, and P. Schniter, "Full-duplex bidirectional MIMO: Achievable rates under limited dynamic range," *IEEE Trans. Signal Process.*, vol. 60, no. 7, pp. 3702-3713, July 2012.
- [10] J. Gorski, F. Pfoeffler, and K. Klamroth, "Biconvex sets and optimization with biconvex functions: a survey and extensions," *Mathematical Methods of Operations Research*, vol. 66, no. 3, pp. 373-407, 2007.
- [11] H. Al-Shatri, X. Li, R. S. Ganesan, A. Klein and T. Weber, "Maximizing the sum rate in cellular networks using multiconvex optimization," *IEEE Trans. Wireless Commun.*, vol. 15, no. 5, pp. 3199-3211, May 2016.
- [12] A. C. Cirik, R. Wang, Y. Hua, and M. Latva-aho "Weighted sum-rate maximization for full-duplex MIMO interference channels," *IEEE Trans. Commun.*, vol. 63, no. 3, pp. 801-815, March. 2015.
- [13] S. S. Christensen, R. Agarwal, E. Carvalho, and J. M. Cioffi, "Weighted sum rate maximization using weighted MMSE for MIMO-BC beamforming design," *IEEE Trans. Wireless Commun.*, vol. 7, pp. 4792-4799, Dec. 2008.
- [14] Q. Shi, M. Razaviyayn, Z.-Q. Luo, C. He, "An iteratively weighted MMSE approach to distributed sum-utility maximization for a MIMO interfering broadcast channel," *IEEE Trans. Signal Process.*, vol. 59, no. 9, pp. 4331-4340, Sep. 2011.
- [15] A. C. Cirik, R. Wang, Y. Rong, and Y. Hua, "MSE-based transceiver designs for full-duplex MIMO cognitive radios," *IEEE Trans. Commun.*, vol. 63, no. 6, pp. 2056-2070, June 2015.
- [16] J. Kaleva, A. Tölli, and M. Juntti, "Decentralized sum rate maximization with QoS constraints for interfering broadcast channel via successive convex approximation," *IEEE Trans. Signal Process.*, vol. 64, no. 11, pp. 2788-2802, June, 2016.
- [17] W. Li, J. Lilleberg, and K. Rikkinen, "On rate region analysis of half- and full-duplex OFDM communication links," *IEEE J. Sel. Areas in Commun.*, vol. 32, no. 9, pp. 1688-1698, Sept. 2014.
- [18] J. Zhang, O. Taghizadeh, and M. Haardt, "Transmit strategies for full-duplex point-to-point systems with residual self-interference," in *Proc. Int. ITG Workshop on Smart Antennas (WSA 2013)*, pp. 1-8, Mar. 2013.

- [19] X. Xia, D. Zhang, K. Xu, W. Ma, and Y. Xu, "Hardware impairments aware transceiver for full-duplex massive MIMO relaying," *IEEE Trans. on Signal Process.*, vol. 63, no. 24, pp. 6565-6580, Dec. 2015.
- [20] T. M. Kim, H. J. Yang, and A. Paulraj, "Distributed sum-rate optimization for full-duplex MIMO system under limited dynamic range," *IEEE Signal Process. Lett.*, vol. 20, no. 6, pp. 555-558, June 2013.
- [21] H. Suzuki, T. V. A. Tran, I. B. Collings, G. Daniels, and M. Hedley, "Transmitter noise effect on the performance of a MIMO-OFDM hardware implementation achieving improved coverage," *IEEE J. Sel. Areas Commun.*, vol. 26, no. 6, pp. 867-876, Aug. 2008.
- [22] W. Namgoong, "Modeling and analysis of nonlinearities and mismatches in AC-coupled direct-conversion receiver," *IEEE Trans. Wireless Commun.*, vol. 4, no. 1, pp. 163-173, Jan. 2005.
- [23] S. Boyd and L. Vandenberghe, *Convex Optimization*. Cambridge University Press, 2004.
- [24] P. Tseng, "Convergence of a block coordinate decent method for non-differentiable minimization," *Journal of optimization theory and applications*, vol. 109, no. 3, pp. 475-494, June 2001.
- [25] S. Goyal, P. Liu and S. Panwar, "User selection and power allocation in full duplex multi-cell networks," *IEEE Trans. Vehicular Tech.*, in press, 2016.
- [26] D. P. Palomar, J. M. Cioffi, and M. A. Lagunas, "Joint Tx-Rx beamforming design for multicarrier MIMO channels: A unified framework for convex optimization," *IEEE Trans. Signal Process.*, vol. 51, no. 9, pp. 2381-2401, Sept 2003.
- [27] 3GPP, TR 36.828, "Further enhancements to LTE time division duplex (TDD) for downlink-uplink (DL-UL) interference management and traffic adaptation (Release 11)," June 2012.
- [28] S. Goyal, P. Liu, S. Panwar, R. DiFazio, R. Yang, J. Li, and E. Bala, "Improving small cell capacity with common-carrier full duplex radios," in *Proc. IEEE Int. Conf. Commun. (ICC 2014)*, pp. 4987-4993, June 2014.
- [29] DUPLO project, "System scenarios and technical requirements for full-duplex concept," Deliverable D1.1. [Online]. Available: <http://www.fp7-duplo.eu/index.php/deliverables>.
- [30] D. Fooladivanda, and C. Rosenberg, "Joint resource allocation and user association for heterogeneous wireless cellular networks," *IEEE Trans. Wireless Commun.* vol. 12, no. 1, pp. 248-257, Jan. 2013.



**Ali Cagatay Cirik** (S'13-M'14) received the B.S and M.S. degrees in telecommunications and electronics engineering from Sabanci University, Istanbul, Turkey, in 2007 and 2009, respectively, and Ph.D. degree in electrical engineering from University of California, Riverside in 2014. He held research fellow positions at Centre for Wireless Communications, Oulu, Finland and Institute for Digital Communications (IDCOM), University of Edinburgh, U.K between June 2014 and November 2015. His industry experience includes internships at Mitsubishi Electric

Research Labs (MERL), Cambridge, MA, in 2012 and at Broadcom Corporation, Irvine, CA, in 2013. Currently, he is working as a research scientist at Sierra Wireless, Richmond, Canada. He is also affiliated with University of British Columbia, Vancouver, Canada. His primary research interests are full-duplex communication, 5G non-orthogonal multiple-access (NOMA), MIMO signal processing, and convex optimization.



**Omid Taghizadeh** received his M.Sc. degree in Communications and Signal Processing in April 2013, from Ilmenau University of Technology, Ilmenau, Germany. From September 2013, he has been a research assistant in the Institute for Theoretical Information Technology, RWTH Aachen University. His research interests include full-duplex wireless systems, MIMO communications, optimization, and resource allocation in wireless networks.



**Lutz Lampe** (M'02-SM'08) received the Dipl.-Ing. and Dr.-Ing. degrees in electrical engineering from the University of Erlangen, Germany, in 1998 and 2002, respectively. Since 2003, he has been with the Department of Electrical and Computer Engineering, The University of British Columbia, Vancouver, BC, Canada, where he is a Full Professor. His research interests are broadly in theory and application of wireless, power line, optical wireless and optical fibre communications. Dr. Lampe was the General (Co-)Chair for 2005 IEEE International Conference

on Power Line Communications and Its Applications (ISPLC), 2009 IEEE International Conference on Ultra-Wideband (ICUWB) and 2013 IEEE International Conference on Smart Grid Communications (SmartGridComm). He is currently an Associate Editor of the IEEE WIRELESS COMMUNICATIONS LETTERS and the IEEE COMMUNICATIONS SURVEYS AND TUTORIALS and has served as an Associate Editor and a Guest Editor of several IEEE transactions and journals. He was a (co-)recipient of a number of best paper awards, including awards at the 2006 IEEE ICUWB, the 2010 IEEE International Communications Conference (ICC), and the 2011 IEEE ISPLC. He is co-editor of the book "Power Line Communications: Principles, Standards and Applications from Multimedia to Smart Grid," published by John Wiley & Sons in its 2nd edition in 2016.



**Rudolf Mathar** received his Ph.D. in 1981 from RWTH Aachen University. Previous positions include lecturer positions at Augsburg University and at the European Business School. In 1989, he joined the Faculty of Natural Sciences at RWTH Aachen University. He has held the International IBM Chair in Computer Science at Brussels Free University in 1999. In 2004 he was appointed head of the Institute for Theoretical Information Technology in the Faculty of Electrical Engineering and Information Technology at RWTH Aachen University. From 1994

to present he held numerous visiting Professor positions at The University of Melbourne, Canterbury University, Christchurch, Johns Hopkins University, Baltimore, and others. In 2002, he was the recipient of the prestigious Vodafone Innovation Award, and in 2010 he was elected member of the NRW Academy of Sciences and Arts. He is co-founder of two spin-off enterprises. From October 2011 to July 2014 he served as the dean of the Faculty of Electrical and Engineering and Information Technology. In April 2012 he was elected speaker of the board of deans at RWTH Aachen University. Since August 2014 he is serving as Pro-rector for research and structure at RWTH Aachen University. His research interests include information theory, mobile communication systems, particularly optimization, resource allocation and access control.



**Yingbo Hua** (S'86-M'88-SM'92-F'02) received a B.S. degree (1982) from Southeast University, Nanjing, China, and a Ph.D. degree (1988) from Syracuse University, Syracuse, NY. He held a faculty position with the University of Melbourne, Australia, where he was promoted to the rank of Reader and Associate Professor from 1996. He was a visiting professor with Hong Kong University of Science and Technology (1999-2000), and a consultant with Microsoft Research, WA (summer 2000). Since 2001, he has been a Professor with the University of California at

Riverside.

Dr. Hua has served as Editor, Guest Editor, Member of Editorial Board and/or Member of Steering Committee for IEEE Transactions on Signal Processing, IEEE Signal Processing Letters, EURASIP Signal Processing, IEEE Signal Processing Magazine, IEEE Journal of Selected Areas in Communications, and IEEE Wireless Communication Letters. He has been a Member of IEEE Signal Processing Society's Technical Committees for Underwater Acoustic Signal Processing, Sensor Array and Multichannel Signal Processing, and Signal Processing for Communication and Networking. He has served on Technical and/or Organizing Committees for over 50 international conferences and workshops. He has authored/coauthored over 300 articles and coedited three volumes of books, with more than 9000 citations, in the fields of Sensing, Signal Processing and Communications. He is a Fellow of IEEE and AAAS.